HYDROLOGICAL PROCESSES
Hydrol. Process. (2015)
Published online in Wiley Online Library
(wileyonlinelibrary.com) DOI: 10.1002/hyp.10566

A coupled hydrology–biogeochemistry model to simulate dissolved organic carbon exports from a permafrost-influenced catchment

Jason S. Lessels,[1]* Doerthe Tetzlaff,[1] Sean K Carey,[2] Pete Smith[3] and Chris Soulsby[1]

[1] *The Northern Rivers Institute, School of Geosciences, University of Aberdeen, Aberdeen, UK*
[2] *School of Geography and Earth Sciences, McMaster University, Hamilton, Ontario, Canada*
[3] *Institute of Biological and Environment Sciences, University of Aberdeen, Aberdeen, UK*

Abstract:

We outline the development of a simple, coupled hydrology–biogeochemistry model for simulating stream discharge and dissolved organic carbon (DOC) dynamics in data sparse, permafrost-influenced catchments with large stores of soil organic carbon. The model incorporates the influence of active layer dynamics and slope aspect on hydrological flowpaths and resulting DOC mobilization. Calibration and evaluation of the model was undertaken using observations from Granger Basin within the Wolf Creek research basin, Yukon, northern Canada. Results show that the model was able to capture the dominant hydrological response and DOC dynamics of the catchment reasonably well. Simulated DOC was highly correlated with observed DOC ($r^2 = 0.65$) for the study period. During the snowmelt period, the model adequately captured the observed dynamics, with simulations generally reflecting the timing and magnitude of the observed DOC and stream discharge. The model was less successful over the later summer period although this partly reflected a lack of DOC observations for calibration. The developed model offers a valuable framework for investigating the interactions between hydrological and DOC processes in these highly dynamic systems, where data acquisition is often very difficult. © 2015 The Authors Hydrological Processes Published by John Wiley & Sons, Ltd.

KEY WORDS coupled model; hydrology; biogeochemistry; DOC; permafrost; sub-arctic

Received 24 November 2014; Accepted 1 June 2015

INTRODUCTION

The Arctic and sub-arctic regions are dominated by permafrost and discontinuous permafrost soils, which contain large stores of soil organic carbon (SOC) (Guo *et al.*, 2007; Schuur *et al.*, 2008). Proportionally large amounts of carbon are released from these catchments via aquatic pathways (Cole *et al.*, 2007; Schuur *et al.*, 2008; Kicklighter *et al.*, 2013) with dissolved organic carbon (DOC) being an important form of carbon in these streams (Cole *et al.*, 2007; Balcarczyk *et al.*, 2009; Cory *et al.*, 2014). Permafrost has a significant influence on hydrological flowpaths (Quinton and Marsh, 1999; Gray *et al.*, 2001; Carey and Woo, 2001) with the thawed active layer controlling the timing of DOC production and exports (Carey, 2003; Guo *et al.*, 2012; Kicklighter *et al.*, 2013). Recent work indicates a deepening of the active layer (Oelke *et al.*, 2004; Quinton *et al.*, 2011; Kicklighter *et al.*, 2013) and the degradation and loss of discontinuous permafrost soils from surface temperature warming, which will have large impacts on both the hydrological and DOC cycles (Dye, 2003; Oelke *et al.*, 2004; Finlay *et al.*, 2006; Cole *et al.*, 2007; McGuire and Anderson, 2009; Quinton *et al.*, 2011; Cory *et al.*, 2014).

Studies investigating the interaction between SOC and aquatic pathways in high latitude areas have often focussed on large pan-arctic catchments (Striegl *et al.*, 2005; Guo *et al.*, 2012; Holmes *et al.*, 2012; Mann *et al.*, 2012; Tank *et al.*, 2012). Understandably, these larger catchments have received greater attention as collectively they represent roughly 10% of the earth's discharge and DOC exports (Guo and Macdonald, 2006; Wickland *et al.*, 2012). These large-scale studies have revealed valuable information on the processes regulating DOC exports in these systems and the underlying controlling factors. Studies focusing on controls of DOC at smaller scales have shown that the export of DOC to streams is influenced by the presence and location of permafrost active layer thaw depth and runoff processes within the catchment (Carey, 2003; Kawahigashi *et al.*, 2004; O'Donnell and Jones, 2006; Petrone *et al.*, 2006; Prokushkin *et al.*, 2007; Koch *et al.*, 2013). Runoff

*Correspondence to: Jason S Lessels, The Northern Rivers Institute, School of Geosciences, University of Aberdeen, Aberdeen, UK.
E-mail: jason.lessels@abdn.ac.uk

generation in high-latitude catchments is strongly influenced by snowmelt processes (Mcnamara *et al.*, 1997; Dornes *et al.*, 2008; Carey and Woo, 2001) with much of the snowmelt entering the stream as overland flow or through the upper organic layer, which is characterized by relatively high infiltration rates (Quinton and Marsh, 1999; Carey and Woo, 2001; Gray *et al.*, 2001; Carey and Quinton, 2005; Koch *et al.*, 2013). Permafrost soil in these regions limits deep drainage, sustaining near surface water tables influencing runoff generation (Mcnamara *et al.*, 1997; Quinton and Marsh, 1999; Carey and Woo, 1999). In addition, the presence of organic soil with high infiltration rates and inter-hummock hollows in the organic layer support dominant near surface flowpaths (Mcnamara *et al.*, 1997; Quinton and Marsh, 1999).

Dissolved organic carbon exports from permafrost-dominated catchments are high during early spring when the thawed active layer is shallow (Carey, 2003; Frey and McClelland, 2009) and soil water is in contact with relatively modern labile forms of SOC (Guo and Macdonald, 2006; Raymond *et al.*, 2007). Later in the season, as the active layer deepens, soil water comes into contact with mineral soils associated with less labile carbon and acts to immobilize DOC via sorption (Lyon *et al.*, 2010; Koch *et al.*, 2013). However, observations of older carbon within stream DOC during late summer (Neff *et al.*, 2006; Guo and Macdonald, 2006) highlight the importance of the contribution of DOC from deeper SOC within mineral soils and often evolved from in-stream processing (Zou *et al.*, 2006). With projections of a loss of areal coverage of permafrost and a deepening of the active layer in sub-arctic regions (Cole *et al.*, 2007; McClelland *et al.*, 2007), it is crucial to understand the interaction between hydrological flowpaths and DOC production and transport from soils to streams, which ultimately enter and influence biogeochemical processes in the Arctic ocean (McClelland *et al.*, 2007; McGuire and Anderson, 2009; Holmes *et al.*, 2012; Cory *et al.*, 2014).

Several studies have modelled the export of DOC in streams across different climatic regions using a variety of model complexity and structures. Linear models are commonly used to estimate DOC in sub-arctic environments based on a proportional relationship between stream discharge and DOC (Carey, 2003; Jutras *et al.*, 2011; Guo *et al.*, 2012). Using this method of statistically based estimation provides an overall understanding of seasonal or annual exports, but only limited understanding of the underlying controlling processes. An alternative approach is the use of physically based models. Several physically based models have been developed to simulate DOC production in soils and are used in conjunction with hydrological models to estimate DOC catchment exports. This approach combines the output from hydrological models with that of terrestrial based soil carbon models, with the hydrological and biogeochemical models calibrated individually. One of the most widely applied of these is the Dynamic DOC model (Michalzik *et al.*, 2003), which combines soil carbon production and loss functions for multiple soil layers and includes a simple hydrological model to simulate soil moisture and runoff processes. Recently, Jutras *et al.* (2011) used the Forest Hydrological model to supply soil temperature and moisture to the biogeochemical based DOC-3 model to simulate DOC exports in 11 catchments in Nova Scotia, Canada. Other DOC models include the Integrated Catchments Model for Carbon (Futter *et al.*, 2007) and the Estimating Carbon in Organic Soils Sequestration and Emissions (ECOSSE) (Smith *et al.*, 2010a,2010b; Abdalla *et al.*, 2014). However, these models aim to represent all organic carbon transformations and, therefore, may be overly complex when trying to simulate DOC dynamics at the headwater scale in high-latitude environments, where data acquisition is often difficult. Alternatively, Birkel *et al.* (2014) and Dick *et al.* (2014) present a parsimonious hydrological–biogeochemical model, which incorporates the main controlling processes to simulate DOC and stream discharge on a daily basis from an upland Scottish catchment. Such use of a parsimonious coupled model provides a framework to identify the dominant processes affecting DOC transport at a catchment scale.

Here, we outline the development and evaluation of a parsimonious hydrological–biogeochemical model based on the dominant processes of DOC production and export to simulate daily DOC and stream discharge in a small, but complex, sub-arctic alpine catchment with permafrost influence.

The specific objectives are as follows:

- Develop and calibrate a simple, coupled hydrological and biogeochemical model to simulate stream discharge and DOC dynamics in a sub-arctic alpine catchment.
- Evaluate the suitability of such coupled models for representing dominant hydrological and biogeochemical processes in these systems.

STUDY SITE AND DATA

The 7.4-km^2 Granger basin is a sub-arctic alpine catchment within the Wolf Creek research basin, Yukon, Canada (Figure 1), with an elevation range of 1310–2250 m.a.s.l. (Quinton *et al.*, 2005). Annual precipitation in the catchment is estimated at 478 mm (Laudon *et al.*, 2012) with strong seasonality and ~50% falling as snow (Carey, 2003). Air temperature varies with a winter and

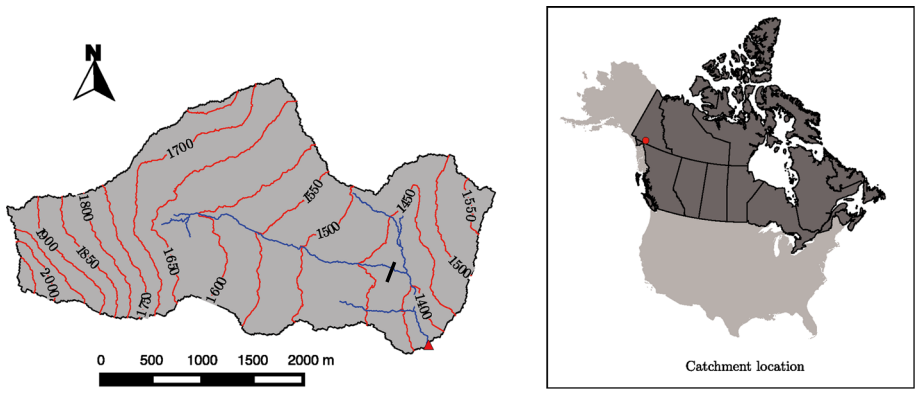

Figure 1. Location and map of study catchment; and locations of the stream gauge at the catchment outlet (red triangle) and of the dip-wells transect (bold black line)

summer mean of −21 and 15 °C, respectively (Carey, 2003). The soils are characterized by 0.05-m to 0.4-m thick organic layers overlying fine to coarse textured colluvium (Carey and Woo, 1999). Permafrost is dominant on north-facing slopes at higher elevations (Carey, 2003; Lewkowicz and Ednie, 2004) with seasonal frost on south-facing slopes. The snow depth, organic layer thickness and presence of permafrost are all heavily dependent on the slope aspect, with thicker organic layers, and higher likelihood of permafrost and late lying deeper snow packs on north-facing slopes throughout the catchment (Carey, 2003; Lewkowicz and Ednie, 2004; McCartney *et al.*, 2006). An estimated 43% of the greater Wolf Creek research basin is underlain by permafrost (Lewkowicz and Ednie, 2004).

Field data used here were collected over a 7-year period with DOC samples collected over 5 years during and after the spring snowmelt period of each year. Stream discharge was measured at the outlet during summer months, with gauging equipment removed during winter months when the stream freezes. A total of 179 DOC stream water samples were collected during the study period. In addition to stream water samples, shallow groundwater DOC samples were collected at several locations along a transect across north-facing and south-facing slopes perpendicular to the main stream with the approximate location of the transect (Figure 3). The shallow groundwater dip-wells were constructed using 35-mm PVC pipe with screen mesh along the entire below surface section to a depth of 0.75 and 1.0 m on the north-facing and south-facing slopes, respectively (Carey, 2003). Sampling of the wells commenced on 9 May 2002 but was later for some wells because of snow cover or lack of water. South-facing slopes averaged 25.8 mg C L^{-1} between 10 and 15 May and later reduced to an average of 7.8 mg C L^{-1} between 1 and 5 June while the north-facing slopes averaged 55.4 mg C L^{-1} between 15 and 20 May and 19.1 mg C L^{-1} during 1 and 5 June (Carey, 2003). Additional information about the DOC samples is provided by Carey (2003). Air temperature and daily rainfall data were obtained from a nearby weather station (c.a. 2.5 km). To fill gaps of missing precipitation and air temperature, additional data were obtained from the meteorological station at Whitehorse airport, located 15 km from the catchment and at an elevation of 706 m.a.s.l. (Carey, 2003). Missing air temperature data were estimated using a linear relationship between the alpine station and Whitehorse airport, while no correction was undertaken for precipitation data. Daily potential evapotranspiration was estimated using the Thornthwaite equation (Thornthwaite, 1948) corrected for daily temperature using the SPEI package (Beguería and Vicente-Serrano, 2013).

THE COUPLED HYDROLOGY-DOC MODEL

A semi-distributed conceptual model was developed to simulate stream discharge and DOC production and loss. The coupled model consists of two parts: a hydrological component using a modified version of the Hydrologiska Byråns Vattenbalansavdelning (HBV) rainfall–runoff model (Lindström *et al.*, 1997) and a DOC production component using a modified version of the DOC production and loss functions based on the algorithms in the ECOSSE soil carbon model (Smith *et al.*, 2007). Figure 2 presents the conceptualization of the two components and how they are linked together. Both model components have been programmed in the R statistical language (R Core Team, 2012) and C++ using the Rcpp (Eddelbuettel and François, 2011) and the RcppArmadillo packages (Eddelbuettel and Sanderson, 2014).

Hydrological model component

The HBV model was further modified to account for the influence of permafrost and seasonal frost on stream discharge. The HBV model has several subroutines that

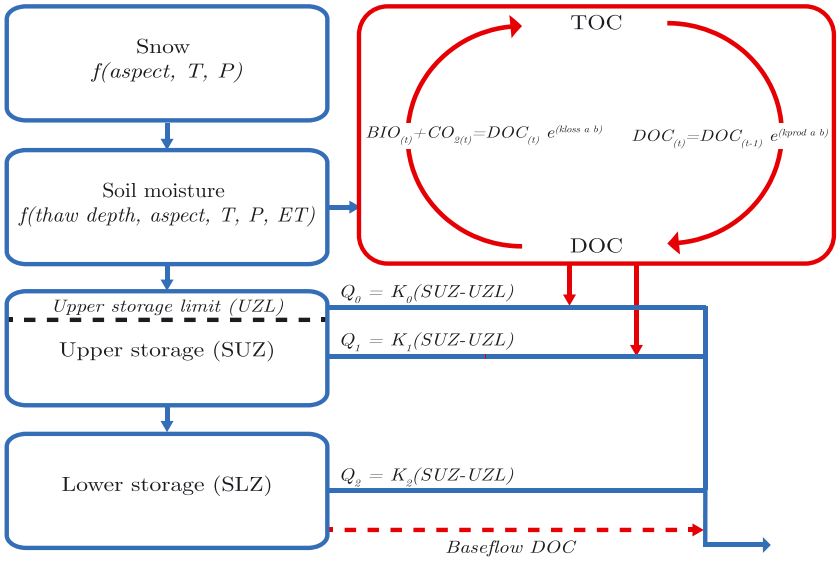

Figure 2. Structure of the coupled hydrological–biogeochemical model. The hydrological components of the model are in blue and the biogeochemical components are in red. The model has two hydrological stores; storage upper zone (SUZ) and storage lower zone (SLZ)

account for snow accumulation and melt, evaporation, soil moisture and runoff described in detail by (Lindström *et al.*, 1997). A description of each coefficient used in the model is outlined in Table I.

Here, we accounted for the effects of aspect on snow accumulation and the onset of snowmelt. On the basis of the work of Hottelet and Braun (1993), the model was applied as a semi-distributed model, separated into three hydrological response units (HRUs) based on aspect: north, south and east–west units. To minimize the number of model coefficients, the same model coefficients were used for all HRUs but were altered by the aspect coefficient of the model. This method modifies the degree-day factor on south-facing slopes by multiplying the degree-day constant (CFMAX) by FASPECT on south-facing slopes and dividing by FASPECT on north-facing slopes (Hottelet and Braun, 1993; Konz and Seibert, 2010). The overall effect of this modification is that north-facing slopes generally have a larger snowpack and the onset of the snowmelt is later than that of south-facing slopes.

In addition, all water storage components have been modified using a degree-day function to incorporate the effect of permafrost and seasonal frost on the hydrology of the catchment. The standard HBV model has three storage components: soil moisture, and upper and lower groundwater storages. On the basis of the work of Heerma (2013), the same degree-day factor used for snowmelt was used to represent the freeze–thaw processes of the permafrost active layer and seasonal frost in each storage component for all three HRUs. Conceptually, the water stored in the ground gradually freezes when the temperature drops below the temperature threshold of the model based on the following equations:

Table I. Description and units of the hydrological model parameters

Model coefficient	Units	Description
TT	°C	Threshold temperature for snow
CFMAX	mm day^{-1}	Degree day coefficient for snow accumulation and freeze–thaw routine of permafrost
SFCF	–	Snowfall correction factor
CFR	–	Refreezing snowmelt parameter
CWH	–	Maximum snowmelt retained by snow pack
FC	mm	Field capacity of soil moisture
BETA	–	Relative contribution to runoff
UZL	mm	Maximum limit of upper storage
K_0	day^{-1}	Upper storage recession parameter (overland flow)
K_1	day^{-1}	Upper storage recession parameter (subsurface flow)
K_2	day^{-1}	Lower storage recession parameter (groundwater)
PERC	mm day^{-1}	Maximum percolation to lower storage
FASPECT	–	Correction coefficient for slope aspect

$$Y_{(t)} = Y_{(t-1)} + CFR \cdot CFMAX \cdot (TT - T_{(t)}) \quad (1)$$

where $Y_{(t)}$ represents the frozen water content of the soil, or upper or lower storage zones. When air temperature is above the threshold, thawing of the three storages commences based on the following equations:

$$Y_{(t)} = Y_{(t-1)} - CFR \cdot CFMAX \cdot (T_{(t)} - TT) \quad (2)$$

This conceptual thaw–freeze process restricts runoff from the upper and lower storages during winter months. To minimize model complexity, the freezing and thawing of these storages are undertaken independent of each other. The freezing of the soil moisture within the model increases the concentration of stored DOC and also limits the production of DOC from the reduction in soil moisture.

Three linear response functions were used: two runoff components for the upper storage, where the first reflects overland flow when the upper storage is at or greater than the field capacity. The second response function reflects the subsurface drainage through the organic layer. The third response function reflects base-flow runoff from deeper storages.

DOC model component

The DOC component of the coupled model consists of a production and loss routine based on the methods used in the ECOSSE soil carbon model (Smith *et al.*, 2007). The coefficients of the biogeochemical component of the model are detailed in Table II. The DOC production function uses a single carbon pool, does not consider temporal inputs from plant material and assumes a static total organic carbon (TOC) pool. Therefore, TOC is the only carbon pool used in this study, and the production rate constant of Smith *et al.* (2007) for the different carbon pools was not used but estimated during model calibration. The initial range of the production coefficient (k_{prod}) was based on the range of the coefficients used for the carbon pools in the ECOSSE model (Table IV). The initial range of the coefficient representing the decomposition to biomass and CO_2 is also provided in Table II. TOC was set at $5.4\,\text{kg}\,\text{m}^2$ for the catchment on the basis of the estimates by Hugelius *et al.* (2013) for the upper 30 cm of the soil profile representing an average for the catchment.

Daily DOC production was estimated on the basis of a combination of the DOC production coefficient and two additional terms using soil moisture, air temperature and a rate constant modifier,

$$\text{DOC}_{(t)} = \text{DOC}_{(t-1)} + \text{TOC}e^{\left(k_{\text{prod}}a_{(t)}b_{(t)}\right)} \tag{3}$$

Table II. Description and units of the DOC model parameters

Model coefficient	Units	Description
$\text{MAXBAS}_{\text{DOC}}$	day^{-1}	Equilateral triangular weight delay function for DOC
TOC	$\text{kg}\,\text{m}^{-2}$	Total organic carbon
K_{prod}	day^{-1}	DOC production coefficient
K_{loss}	day^{-1}	DOC loss coefficient
BF	$\text{mg}\,\text{L}^{-1}$	Base-flow concentration

where k_{prod} represents the production rate constant (estimated during calibration), TOC is the total organic carbon ($\text{kg}\,\text{m}^{-2}$) in the upper 30 cm of the soil, and the rate modifiers, a and b, are reflective of the air temperature and soil moisture, respectively. Therefore, DOC production was assumed to be dominant in the upper 30 cm of the soil profile similar to Michalzik *et al.* (2003) and Smith *et al.* (2007). The temperature rate modifier was a based on a Q_{10} temperature coefficient relationship with air temperature where

$$a_{(t)} = 2^{\left(\frac{\text{T}_{(t)}}{10}\right)} \tag{4}$$

and $\text{T}_{(t)}$ is the air temperature at time t. A fixed Q_{10} rate of 2 was used to minimize model complexity, which is commonly used in soil carbon models (Tjoelker *et al.*, 2001) and falls within the range of Q_{10} rates observed in Arctic soils (Lenton and Huntingford, 2003). With a value of 2, the effect of the temperature rate modifier $a_{(t)}$ doubles for every 10-°C temperature increase. This was also used by Michalzik *et al.* (2003) for DOC production simulations within the Dynamic DOC model. The rate modifier for soil moisture was based on that of ECOSSE (Smith *et al.*, 2007), but altered for use with the hydrological model rather than the physically based model used in ECOSSE

$$b_{(t)} = 1 + (1 - 0.2)\left(\frac{\left(\text{SM}_{(t)} - \text{FC}\right)}{\text{FC}}\right) \tag{5}$$

where $SM_{(t)}$ is the soil moisture at time t and FC is the estimated field capacity. The loss of DOC from decomposition into biomass was based on the functions of ECOSSE where

$$\text{BIO}_{(t)} = \text{DOC}_{(t)}e^{\left(k_{\text{loss}}a_{(t)}b_{(t)}\right)} \tag{6}$$

and any decomposition of DOC is assumed to be lost to CO_2 or sorbed to the mineral soil.

Model calibration

Model calibration was performed using the Generalized Likelihood Uncertainty Estimate methodology (Beven and Binley, 1992). Many goodness-of-fit measures have limitations; for example, the Nash–Sutcliffe Efficiency measure is the most commonly used likelihood function applied in conjunction with Generalized Likelihood Uncertainty Estimate (Schoups and Vrugt, 2010) but is explicitly biassed towards high flows (Criss and Winston, 2008; Gupta *et al.*, 2009). This is problematic in calibrating hydrological models in alpine catchments with large snowmelt flows and long periods of winter base-flow conditions (Hamilton *et al.*, 2000). Therefore,

two different measures of model efficiency were used in the models objective function. The Volumetric Efficiency (VE) (Criss and Winston, 2008) was used instead of the Nash–Sutcliffe Efficiency to minimize the effect of large flows on model performance. In addition, the coefficient of determination (r^2) multiplied by the slope of the regression (Br^2) (Krause *et al.*, 2005) between the observed and the predicted values was also used to evaluate the model efficiency for stream discharge. The use of Br^2 was chosen in this study as it was found to provide a more robust representation of the relationship between the simulated and observed values and less susceptible to larger observed values. DOC simulations were also evaluated by Br^2 as this provided a more robust measure compared with the r^2. The three model efficiency measures were combined to formulate a single objective function,

$$\mathrm{OF} = \frac{\mathrm{VE}(Q) + \mathrm{B}r^2(Q) + \mathrm{B}r^2(\mathrm{DOC})}{3} \tag{7}$$

We based calibration on hydrological data from 2001 to 2003 and DOC observations collected during the summers of 2002 and 2003. Because of a limited amount of available data during winter flows when the stream freezes, calibration of stream discharge and DOC was restricted to summer periods where daily stream discharge observations were made. As the TOC and hydrological storages of the model are dynamic in nature, a spin-up period of 40 years was used to initialize the model. This long spin-up period was chosen to ensure the model was in a steady state prior to the study period. A Monte Carlo approach was then used to evaluate a suitable range of model coefficients using 10^6 model evaluations. The behavioural parameter set chosen on the basis of the 0.95 percentile of the objective function and corresponded to the best 50 000 parameter sets.

To investigate the sensitivity and influence of the model coefficients on the simulations, a global sensitivity analysis was conducted. The sensitivity analysis was undertaken using the Latin Hypercube one-factor-at-a-time method proposed by van Griensven *et al.* (2006) as programmed in the hydroPSO R package (Zambrano-Bigiarini and Rojas, 2013). This procedure uses an efficient Latin Hypercube sampling technique to evaluate the model efficiency over the range of the model coefficients to provide a rank of importance for each model coefficient.

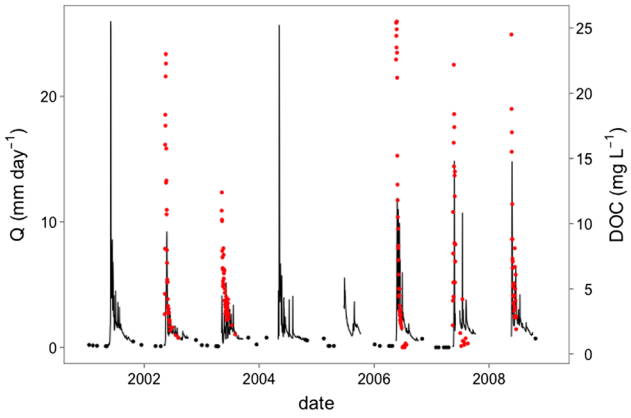

Figure 3. Observed stream discharge (black) and DOC (red points) during the study period. Black points are manually gauged stream discharge measurements made during winter months

OBSERVED HYDROLOGICAL AND DOC DYNAMICS

Figure 3 shows the observed stream discharge and DOC concentrations for the period between 2001 and 2008. Stream discharge is highest during the snowmelt period and then decreases throughout summer; this trend continues until early winter. During this period, stream discharge is responsive to large rainfall events, which results in large discharge peaks later in the season (e.g. 2006 and 2007). Table III provides a summary of annual statistics of stream discharge. Minimum daily discharge is less than 1 mm day^{-1} for each year, and mean discharge is less than 2 mm day^{-1}. There are large inter-annual variations in maximum stream discharge with a range of 5.2–25.7 mm day^{-1} across the study period. As with

Table III. Summary statistics of observed DOC and stream discharge for during the study period

		DOC (mg L^{-1})			Stream discharge (mm day^{-1})		
Year	*n*	Minimum	Mean	Maximum	Minimum	Mean	Maximum
2001					0.1	2.0	26.0
2002	35	1.2	7.8	23	0.1	1.3	9.2
2003	47	1.5	5	12.4	0.1	1.2	5.2
2006	40	0.5	8.6	25.5	0.1	2.0	11.9
2007	26	0.6	7.8	22.2	0.0	1.9	14.9
2008	31	1.9	7.05	24.5	0.7	2.2	14.8

discharge, the highest DOC concentrations are closely linked to the snowmelt runoff period with the observed DOC peak occurring during the snowmelt event before but prior to the peak of stream discharge. DOC concentrations vary from 0.5 to 25.5 mg L^{-1} throughout the study period (Table III). Of the 6 years of DOC observations, only one year (2003) did not have any samples greater than 20 mg L^{-1}.

Simulation of hydrological dynamics

Table IV summaries the model efficiency measures for each year during the study period. There is a wide range in the model efficiencies for each year with all years having a Br^2 = 0. This indicates that for the models accepted as behavioural, many have parameter sets that perform poorly. Similarly, a wide range of model performance is given by the VE measures of each year. On the basis of the model efficiencies, the model performed best during 2008 and poorest during 2003.

Table V provides the initial range and estimated posterior mean and range for each model coefficient. In addition, the table also provides an estimate of the sensitivity of each coefficient. Of the hydrological model coefficients, the snowfall correction factor (SFCF) was found to be the most influential to the model simulations. Hydrological runoff coefficients k1 and UZL were the least important coefficients in the model, indicating that the quick runoff component of the model has little influence on the hydrological responses in the model.

Figure 4 shows the simulated stream discharge for the calibration period (2001–2003) with 90% uncertainty bands. The simulations capture the observed stream discharge dynamics in each year quite well although there are differences. Simulation results are satisfactory, considering the simplicity (low parameter numbers) of the model applied, with no systematic overestimations or underestimations. The simulated discharge during 2001 matches the observed onset of the spring melt event adequately, but the mean simulated maximum peak is not as high as the observed peak. Observed peak discharge during the spring melt is 26 mm day^{-1} and does fall

Table V. Summary of initial and posterior model coefficient distribution ranges determined by Monte Carlo analysis and sensitivity rank of each model coefficient determining using Latin Hypercube one-factor-at-a-time

Model coefficient	Initial range	Posterior mean (10th, 90th percentiles)	Sensitivity rank (normalized relative importance)
K_{loss}	0.005–0.5	0.3 (0.1–0.4)	1 (0.21)
SFCF	0.1–5	2.8 (1.6–4.1)	2 (0.14)
FC	100–500	336.5 (179.8–471.8)	3 (0.14)
CFMAX	1–5	2.2 (1.1–3.7)	4 (0.11)
$MAXBAS_{DOC}$	1–5	3.3 (1.6–4.7)	5 (0.1)
K_{prod}	5e-06–5e-04	0 (0–0)	6 (0.08)
BETA	0.1–5	2.3 (0.6–4.3)	7 (0.07)
K_1	0.01–0.5	0.2 (0.1–0.4)	8 (0.06)
TT	−3–3	−0.9 (−2.5–1)	9 (0.04)
K_2	0.001–0.5	0.2 (0–0.4)	10 (0.03)
PERC	1–10	5.7 (2–9.2)	11 (0.02)
UZL	1–50	26.6 (7.3–45.4)	12 (0.01)
K_0	0.1–0.99	0.5 (0.2–0.9)	13 (0.01)

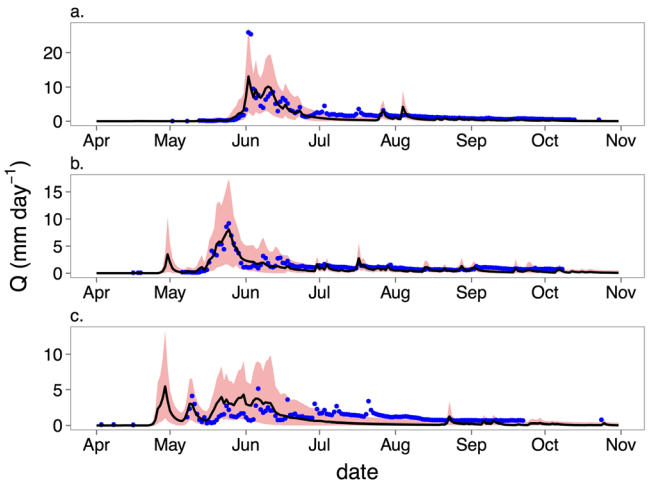

Figure 4. Mean simulated discharge with observed discharge during calibration period for each year: (a) 2001, (b) 2002 and (c) 2003. Blue points indicate observed stream discharge, the solid black line is the mean simulated stream discharge, and the red band is the 90% uncertainty estimates

Table IV. Model efficiency measures of the behavioural parameter set for DOC and stream discharge

	DOC (Br2)			Stream discharge (Br2, VE)		
Year	Minimum	Mean	Maximum	Minimum	Mean	Maximum
2001				0, −0.01	0.33, 0.34	0.74, 0.71
2002	0	0.21	0.93	0, −0.28	0.42, 0.36	0.86, 0.76
2003	0	0.34	0.92	0, −0.74	0.08, 0.05	0.34, 0.68
2006	0	0.38	0.97	0, 0.6	0.4, 0.28	0.84, 0.75
2007	0	0.25	0.84	0, −1.7	0.24, 0.22	0.74, 0.78
2008	0	0.34	0.91	0, −0.6	0.4, 0.21	0.9, 0.84

within the 90% uncertainty bounds of the simulated discharge. The simulated discharge during 2002 indicates a small event prior spring melt runoff, which was not observed. After this small runoff event, a larger observed runoff event is matched closely by the simulated discharge. Dynamics in 2003 are captured well. Stream discharges after the spring melt are underestimated for each year, but the observed discharge does fall within the uncertainty bounds.

Figure 5 presents simulated and observed stream discharges during the years 2006–2008 to test the model on data not used in the calibration. The simulated discharge dynamics closely follow that of the observed stream discharge for each year. Onset and magnitude of the spring melt event of the simulated discharge closely resembles that of the observed discharge for all 3 years. During this period, the simulated discharge peaks resulting from rainfall events later in the season closely resemble the observed stream discharge, with all discharge observations falling within the uncertainty bounds of the simulations.

Simulation of DOC dynamics

For the calibration period, in 2002, the mean simulated DOC shows two concentration peaks coinciding with the spring melt event (Figure 6). There are no observed DOC samples during the first simulated DOC peak, and on the basis of direct field observations, the first sampled DOC during this year captured the spring melt event. The simulated DOC is similar to that of the observed DOC, but occurs before the observed DOC event, possibly due to the small simulated stream discharge event prior to the actual observed snowmelt event, which was most likely

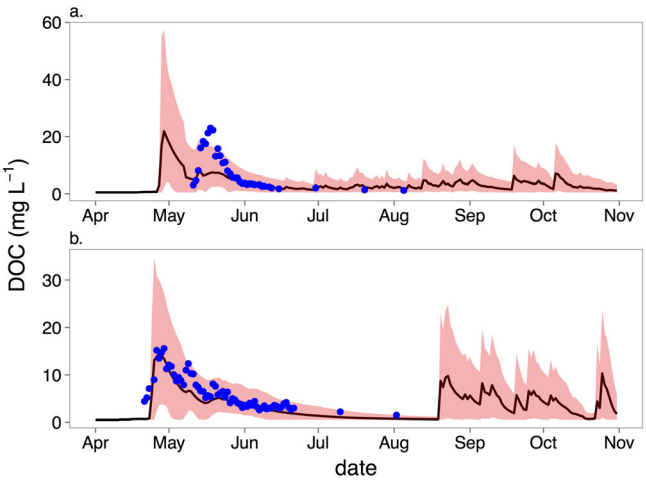

Figure 6. Mean simulated DOC and observed DOC for each year of the calibration period: (a) 2002 and (b) 2003. Blue points indicate observed DOC, the solid black line is the mean simulated DOC, and the red band is the 90% uncertainty estimates

caused by a short period of above-freezing air temperatures. In contrast, the simulated DOC for 2003 closely resembles the dynamics of the observed with the majority of observations falling within the bounds of the simulated uncertainty.

Figure 7 shows the model tests for the years not used in calibration. Simulations generally follow the dynamics of observed DOC for all 3 years. The commencement of the simulated exports of the spring event matches that of the observed DOC. The duration of the simulated spring event is also similar to the observed, but the maximum simulated DOC is consistently below that observed. However, the majority of observed DOC samples fall within the simulated uncertainty bounds for all 3 years.

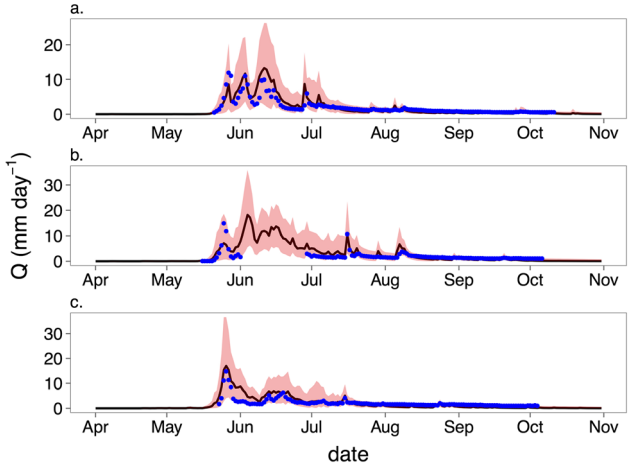

Figure 5. Mean simulated stream discharge with observed stream discharge for each year of the non-calibration period: (a) 2006, (b) 2007 and (c) 2008. Blue points indicate observed stream discharge, the solid black line is the mean simulated stream discharge, and the red band is the 90% uncertainty estimates

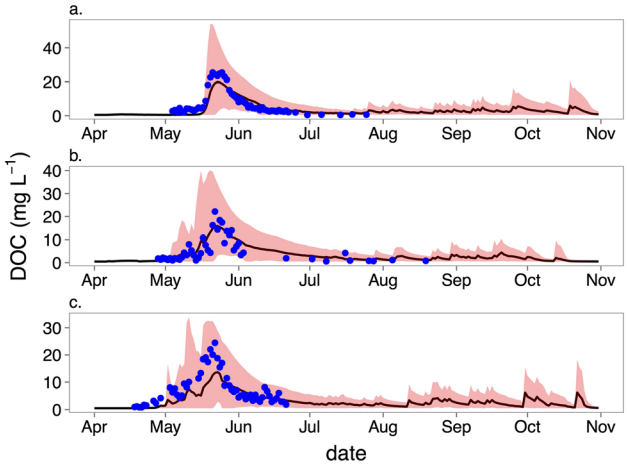

Figure 7. Mean simulated DOC and observed DOC for each year of the non-calibration period: (a) 2006, (b) 2007 and (c) 2008. Blue points indicate observed DOC, the solid black line is the mean simulated DOC, and the red band is the 90% uncertainty estimates

For all 5 years (including the calibration period), simulated DOC concentrations show high variability associated with smaller runoff events during the end of the summer period, which were not captured during field campaigns. Uncertainty bounds are greatest during the recession of the spring melt event and later in the season where there are very few observations.

Dissolved organic carbon production in the model occurs within the soil storage (Figure 2) and is controlled by soil water content and air temperature. Figure 8 shows the mean simulated DOC for the south-facing and north-facing slopes with observed DOC samples collected from dip wells during 2002. Simulated DOC accumulates during the winter period as the amount of frozen soil water increases and is higher at the south-facing slope. The rapid reduction in the concentration of soil water DOC in both slopes shown in the observed dip-well samples is well captured with the simulations. After this rapid flushing of soil water DOC, the concentration of DOC in the soil water increases again over the remaining summer months. During the snowmelt event, DOC is observed to reach a maximum concentration during the rising limb of the freshet hydrograph. Figure 9 shows the simulated and observed stream runoff and DOC exports during 2008. The simulations of the model closely resemble the dynamics of the observed stream discharge and DOC. Simulated DOC peaked during the snowmelt period on the rising limb of the stream discharge.

Overall, the model simulated DOC relatively well during the study period, but there was a wide range of model performances (Table IV). The model efficiency measures show that the model performed best in 2008 and had least skill in 2007. However, the relationship between the observed and mean simulated DOC for all 5 years shows a strong correlation ($r^2 = 0.65$, Figure 10). Simulations tend to underestimate DOC at higher concentrations, corresponding with DOC exports during the spring melt periods. The results of the sensitivity analysis (Table V) showed that K_{loss} was the most sensitivity model coefficient for the simulations while the distribution of the coefficient was quite narrow. In contrast, the production coefficient (K_{prod}) was not as important (ranked 6).

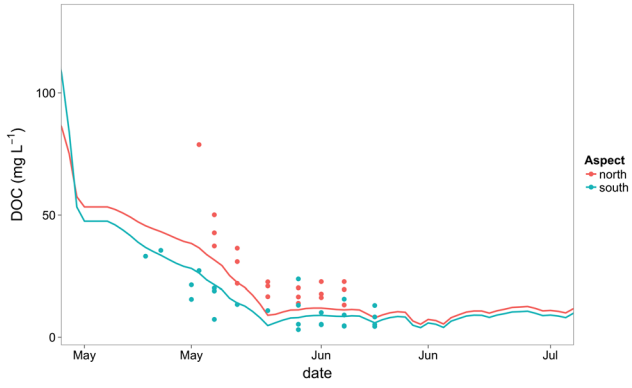

Figure 8. Mean simulated soil water DOC (lines) for north-facing and south-facing slopes with observed DOC (points) from dip-well measurements during 2002

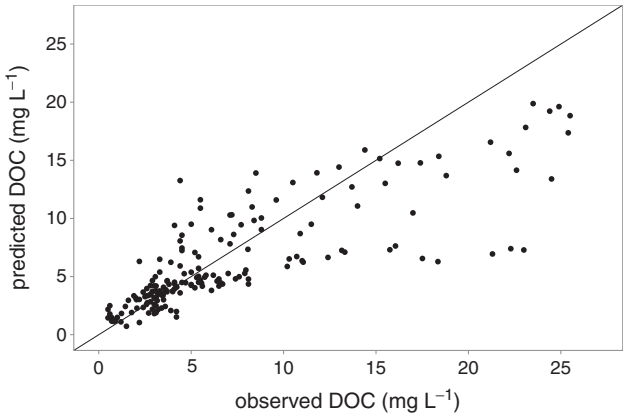

Figure 10. Observed DOC against mean simulated DOC for entire study period ($r^2 = 0.65$)

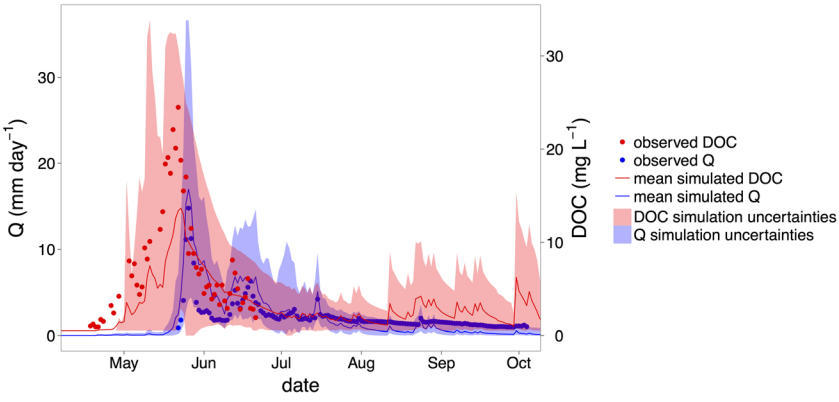

Figure 9. Mean simulated and observed DOC and stream discharge during 2008

DISCUSSION AND WIDER IMPLICATIONS

Understanding the main controlling processes on stream discharge and DOC exports from sub-arctic catchments using a coupled hydrological–biogeochemical model

High-latitude regions are highly vulnerable to climate change and are predicted to lose significant proportions of permafrost. It is widely understood that permafrost, seasonal soil frost and slope aspect have a large influence on the hydrology in these catchments (Quinton and Marsh, 1999; Carey and Woo, 2001; Quinton *et al.*, 2005). In addition, biogeochemical processes controlling the production and export of DOC are closely linked to the hydrological processes of the catchment (Carey, 2003; Lyon *et al.*, 2010; Koch *et al.*, 2013). High-latitude catchments experience strong seasonality, and this seasonality is present in the processes and dynamics of the production and export of DOC, where soil moisture and temperature are the major controls.

In this study, a coupled hydrological–biogeochemical model has been developed to simulate stream discharge and DOC exports in a sub-arctic headwater catchment, based on the perceived dominant controlling processes while minimizing model complexity. The model (Figure 2) presents a simple representation of the dominant hydrological and DOC processes in the catchment. The model builds on the standard HBV model (Lindström *et al.*, 1997) by including components to represent the effects of permafrost, seasonal soil frost and aspect on the hydrological dynamics. In addition, the model incorporates DOC production and loss processes, which are controlled by functions of soil moisture and air temperature.

By including slope aspect and soil freeze–thaw processes, the hydrological component of the model was able to adequately simulate spring melt event duration and magnitude, inter-annual differences of event magnitude and dynamics in late summer, and early autumn and low flows during the winter months. Furthermore, the dynamics of the simulated DOC matched observed DOC concentrations quite well for most study years ($r^2 = 0.65$ for all years). Despite difficulties in simulating the timing and the magnitude of some of the spring melt events, the observations of each year were within the simulated uncertainty bounds (Figure 3).

During winter, stream discharge is very low because of the presence of permafrost, seasonal frost and a reduction in overall storage. As snowmelt begins, melt water infiltrates into highly permeable organic soils and transports the soil water DOC to the stream. Runoff during the snowmelt event is generally the largest observed throughout the year and leads to the highest stream water DOC concentrations (Carey, 2003; Koch *et al.*, 2013). As the summer season progresses, soil thaw increases and allows for the infiltration of water into the deeper mineral soils, which reduces the soil moisture in the upper soils associated with DOC production (Lyon *et al.*, 2010; Koch *et al.*, 2013). However, model simulations showed that the system remains highly responsive to rainfall events as storage is limited because of the presence of permafrost, which leads to increases in DOC stream concentrations.

In many high-latitude and alpine energy limited systems, the timing of hydrological and biogeochemical processes are dependent on the hillslope aspect, with south-facing slopes experiencing snowmelt and soil thaw before north-facing slopes (Boyer *et al.*, 2000; Dornes *et al.*, 2008; Kicklighter *et al.*, 2013). The model developed here was useful to investigate the role of aspect on DOC production. The simulated DOC in soil water at north-facing and south-facing slopes closely resembled the observations in 2003 (Figure 8), with a rapid reduction in DOC associated with the spring melt, supporting previous research indicating that soil moisture and air temperature as dominant controls of DOC production (Michalzik *et al.*, 2003).

Development and calibration of a simple, coupled hydrological and biogeochemical model

Studies modelling stream water DOC commonly calibrate model parameters of hydrological and biogeochemical model components separately to identify the best hydrological and biogeochemical model parameter sets (Michalzik *et al.*, 2003; Futter *et al.*, 2007; Jutras *et al.*, 2011). Here, we used a multi-objective function including hydrological and biogeochemical model efficiencies simultaneously. The aim of this approach was not to identify a single optimal solution but find a range of plausible parameters for each of the two model components (Birkel *et al.*, 2014; Dick *et al.*, 2014). Stream discharge in regions influenced by snowmelt and permafrost varies greatly throughout the year, with very low flows during winter and very large flows occurring over short periods during the spring melt event, making calibration a challenge (Hamilton, 2001). Using a combination of model efficiency other than the commonly used Nash–Sutcliffe measure, which is biassed towards peak observations, Criss and Winston (2008) and Gupta *et al.* (2009) allowed for identification of a suitable parameter range for the hydrological component, which does not bias the results of model calibration towards high flow periods.

One of the largest limitations of model development and calibration for hydrological and biogeochemical processes in high-latitude headwater catchments is the lack of empirical observations (Tetzlaff *et al.*, 2014). Data in these regions is limited because of the difficulties in the

collection of observations in these remote areas (Bishop *et al.*, 2008; Holmes *et al.*, 2008) including technical, logistical and financial constraints. Many studies have focussed on the spring melt period because the majority of stream discharge and DOC is exported during this short time (Carey, 2003; McClelland *et al.*, 2007). In our study, DOC observations were restricted to early spring periods associated with the freshet. We acknowledge that by only having observations of DOC during the spring melt, the calibrated parameter range of the model may not reflect processes operating during late summer and autumn, limiting its applicability during this time. However, the ability of the model to reflect the processes during spring and early summer does support the model structure.

The behavioural parameter sets of the coupled model (Table IV) showed a large range of model efficiency measures for DOC and stream discharge individually, which are associated with the large uncertainty bounds during the spring melt period. In addition, the sensitivity analysis revealed that the K_{loss} coefficient was the most sensitive. The K_{loss} coefficient is used to restrict the accumulation of DOC in storage (Equation (6)). As the catchment undergoes substantial accumulation of DOC over the winter period, it is important that the conversion of DOC to other forms of carbon is correctly balanced with the production of DOC, and this assumption is shown by the sensitivity of this coefficient. However, the model was able to capture the main dynamics of both DOC and stream discharge throughout the study period.

Simulated stream discharge reflected the strong snowmelt influence observed during each spring and simulated stream DOC peaked during the stream discharge rising limb (e.g. Figure 9), which has been observed in this system (Carey, 2003). This strong influence of the snowmelt on the system is also reflected in the sensitivity analysis with the SFCF being the second most-important coefficient. The sensitivity of the SFCF is expected as this parameter was used to correct for the potential underestimation of observed snowfall. These results highlight the difficulty of calibrating hydrological and biogeochemical processes in these systems where extreme events (spring melt) have a large influence on the measures of goodness of fit used in the calibration process.

Evaluation of coupled models for representing dominant hydrological and biogeochemical processes

Modelling provides a framework to help overcome the lack of empirical information and to test hypotheses regarding the dominant controls of hydrology and biogeochemistry in these systems. With limited data to inform the modelling, it is important that the output and complexity of the model is appropriate to the data available (Beven and Freer, 2001; Beven, 2006). The coupled parsimonious model developed here captures the main dynamics seen in the system quite well with a $r^2 = 0.65$ for all DOC observations and a maximum VE of 0.65 for a simulated realization of discharge within each year. Importantly, the model captures prediction of DOC dynamics prior to hydrological events, which is beyond the skill of simple regression based models.

Our model provides a potential framework that could be used to examine the possible effects of climate change in these regions. There are, however, limitations as results suggest that the model struggles to capture the precise timing and magnitude of the spring melt event. In addition, the simulations of both DOC and stream discharge are often associated with large uncertainties. More research is required to investigate the controls of these processes at different scales, focussing on the processes controlling both DOC and stream discharge in these regions. Furthermore, DOC observations are required during late summer to confirm the model DOC simulations. These limitations highlight the difficulties of capturing the dominant processes in complex systems; however, this should not deter the use of models to investigate the controls in these systems.

CONCLUSION

The extent of permafrost in high-latitude regions is predicted to decrease due to climate warming (McGuire and Anderson, 2009; Schaefer *et al.*, 2011). The effect of these changes on hydrological and DOC dynamics in headwaters remains unclear, and it is important that the dominant controls are understood to assess the potential impact of these changes (Kawahigashi *et al.*, 2004; McClelland *et al.*, 2007). In remote headwater catchments in such high-latitude environments, the collection of data is often challenging, and most studies must rely on limited data to investigate the dominant biogeochemical and hydrological processes.

We presented a coupled hydrological–biogeochemical model to simulate discharge and DOC dynamics in high-latitude headwaters. Results show that the parsimonious model was able to capture the dominant controls on stream discharge and DOC in this headwater catchment. However, future work is required to help reduce the uncertainty in both hydrological and biogeochemical components. This could be achieved, for example, by developing models that incorporate information gained from using hydrological tracers for this region. In addition, observations should be expanded to capture DOC exports during late season.

ACKNOWLEDGEMENTS

We thank the Natural Environment Research Council (project NE/K000268/1) and the Natural Sciences and Engineering Research Council of Canada (Changing Cold Regions Network) for funding. We would also like to thank Richard Janowicz from Yukon Environment for the provision of the stream flow data used in this study.

REFERENCES

Abdalla M, Hastings A, Bell MJ, Smith JU, Richards M, Nilsson MB, Peichl M, Löfvenius MO, Lund M, Helfter C, Nemitz E, Sutton MA, Aurela M, Lohila A, Laurila T, Dolman AJ, Belelli-Marchesini L, Pogson M, Jones E, Drewer J, Drosler M, Smith P. 2014. Simulation of CO2 and attribution analysis at six European peatland sites using the ECOSSE model. *Water, Air, and Soil Pollution* **225**: 1–14.

Balcarczyk KL, Jones JB, Jaffé R, Maie N. 2009. Stream dissolved organic matter bioavailability and composition in watersheds underlain with discontinuous permafrost. *Biogeochemistry* **94**: 255–270. DOI: 10.1007/s10533-009-9324-x

Beguería S, Vicente-Serrano SM. 2013. SPEI: Calculation of the Standardised Precipitation–Evapotranspiration Index.

Beven K. 2006. Searching for the Holy Grail of scientific hydrology: $Q_t = (S, R, \Delta t)A$ as closure. *Hydrology and Earth System Sciences* **10**: 609–618. DOI: 10.5194/hess-10-609-2006

Beven K, Binley A. 1992. The future of distributed models: model calibration and uncertainty prediction. *Hydrological Processes* **6**: 279–298.

Beven K, Freer J. 2001. Equifinality, data assimilation, and uncertainty estimation in mechanistic modelling of complex environmental systems using the GLUE methodology. *Journal of Hydrology* **249**: 11–29.

Birkel C, Soulsby C, Tetzlaff D. 2014. Integrating parsimonious models of hydrological connectivity and soil biogeochemistry to simulate stream DOC dynamics. *Journal of Geophysical Research, Biogeosciences* **119**: 1030–1047. DOI: 10.1002/2013JG002551

Bishop K, Buffam I, Erlandsson M. 2008. Aqua Incognita: the unknown headwaters. *Hydrological Processes* **22**: 1239–1242. DOI: 10.1002/hyp.7049

Boyer EW, Hornberger GM, Bencala KE, McKnight DM. 2000. Effects of asynchronous snowmelt on flushing of dissolved organic carbon: a mixing model approach. *Hydrological Processes* **14**: 3291–3308. DOI: 10.1002/1099-1085(20001230)14:18<3291::AID-HYP202>3.0.CO;2-2

Carey S, Woo M. 1999. Hydrology of two slopes in subarctic Yukon, Canada. *Hydrological Processes* **2562**: 2549–2562.

Carey S, Woo M. 2001. Slope runoff processes and flow generation in a subarctic, subalpine catchment. *Journal of Hydrology* **253**: 110–129.

Carey SK. 2003. Dissolved organic carbon fluxes in a discontinuous permafrost subarctic alpine catchment. *Permafrost and Periglacial Processes* **14**: 161–171. DOI: 10.1002/ppp.444

Carey SK, Quinton WL. 2005. Evaluating runoff generation during summer using hydrometric, stable isotope and hydrochemical methods in a discontinuous permafrost alpine catchment. *Hydrological Processes* **19**: 95–114. DOI: 10.1002/hyp.5764

Cole JJ, Prairie YT, Caraco NF, McDowell WH, Tranvik LJ, Striegl RG, Duarte CM, Kortelainen P, Downing JA, Middelburg JJ, Melack J. 2007. Plumbing the global carbon cycle: integrating inland waters into the terrestrial carbon budget. *Ecosystems* **10**: 172–185. DOI: 10.1007/s10021-006-9013-8

Cory RM, Ward CP, Crump BC, Kling GW. 2014. Sunlight controls water column processing of carbon in arctic fresh waters. *Science* **345**: 925–928. DOI: 10.1126/science.1253119

Criss R, Winston W. 2008. Do Nash values have value? Discussion and alternate proposals. *Hydrological Processes* **2725**: 2723–2725. DOI: 10.1002/hyp

Dick JJ, Doerthe T, Birkel C, Soulsby C. 2014. Modelling landscape controls on dissolved organic carbon sources and fluxes to streams. *Biogeochemistry*. DOI: 10.1007/s10533-014-0046-3

Dornes PF, Pomeroy JW, Pietroniro A, Carey SK, Quinton WL. 2008. Influence of landscape aggregation in modelling snow-cover ablation and snowmelt runoff in a sub-arctic mountainous environment. *Hydrological Sciences Journal* **53**: 725–740. DOI: 10.1623/hysj.53.4.725

Dye DG. 2003. Seasonality and trends of snow-cover, vegetation index, and temperature in northern Eurasia. *Geophysical Research Letters* **30**: 1405. DOI: 10.1029/2002GL016384

Eddelbuettel D, François R. 2011. Rcpp: seamless R and C++ integration. *Journal of Statistical Software* **40**: 1–18.

Eddelbuettel D, Sanderson C. 2014. RcppArmadillo: accelerating R with high-performance C++ linear algebra. *Computational Statistics and Data Analysis* **71**: 1054–1063. DOI: 10.1016/j.csda.2013.02.005

Finlay J, Neff J, Zimov S, Davydova A, Davydov S. 2006. Snowmelt dominance of dissolved organic carbon in high-latitude watersheds: Implications for characterization and flux of river DOC. *Geophysical Research Letters* **33**. DOI: 10.1029/2006GL025754

Frey K, McClelland J. 2009. Impacts of permafrost degradation on arctic river biogeochemistry. *Hydrological Processes* **23**: 169–182. DOI: 10.1002/hyp

Futter MN, Butterfield D, Cosby BJ, Dillon PJ, Wade AJ, Whitehead PG. 2007. Modeling the mechanisms that control in-stream dissolved organic carbon dynamics in upland and forested catchments. *Water Resources Research* **43**. DOI: 10.1029/2006WR004960

Gray DM, Toth B, Zhao L, Pomeroy JW, Granger RJ. 2001. Estimating areal snowmelt infiltration into frozen soils. *Hydrological Processes* **15**: 3095–3111. DOI: 10.1002/hyp.320

Guo L, Cai Y, Belzile C, Macdonald RW. 2012. Sources and export fluxes of inorganic and organic carbon and nutrient species from the seasonally ice-covered Yukon River. *Biogeochemistry* **107**: 187–206. DOI: 10.1007/s10533-010-9545-z

Guo L, Macdonald RW. 2006. Source and transport of terrigenous organic matter in the upper Yukon River: Evidence from isotope (δ 13 C, Δ 14 C, and δ 15 N) composition of dissolved, colloidal, and particulate phases. *Global Biogeochemical Cycles* **20**. DOI: 10.1029/2005GB002593

Guo L, Ping C-L, Macdonald RW. 2007. Mobilization pathways of organic carbon from permafrost to arctic rivers in a changing climate. *Geophysical Research Letters* **34**. DOI: 10.1029/2007GL030689

Gupta HV, Kling H, Yilmaz KK, Martinez GF. 2009. Decomposition of the mean squared error and NSE performance criteria: implications for improving hydrological modelling. *Journal of Hydrology* **377**: 80–91. DOI: 10.1016/j.jhydrol.2009.08.003

Hamilton AS, DG Hutchinson, RD Moore. 2001. Estimation of winter streamflow using a conceptual hydrological model: a case study, Wolf Creek, Yukon Territory. *Proceedings 11th Workshop on River Ice. River ice processes within a changing environment. Canada Committee on River Ice Processes and the Environment*. CGU-HS: Ottawa, Canada.

Hamilton BAS, Hutchinson DG, Moore RD, Canada E. 2000. Estimating winter streamflow using conceptual streamflow model. *Journal of Cold Regions Engineering* **14**: 158–175.

Heerma K. 2013. Hydrological modeling of a Mongolian River basin under current and changed climate conditions using permafrost conceptualizations. Master Thesis. University of Twente.

Holmes RM, McClelland JW, Peterson BJ, Tank SE, Bulygina E, Eglinton TI, Gordeev VV, Gurtovaya TY, Raymond PA, Repeta DJ, Staples R, Striegl RG, Zhulidov AV, Zimov SA. 2012. Seasonal and annual fluxes of nutrients and organic matter from large rivers to the Arctic Ocean and surrounding seas. *Estuaries and Coasts* **35**: 369–382. DOI: 10.1007/s12237-011-9386-6

Holmes RM, McClelland JW, Raymond PA, Frazer BB, Peterson BJ, Stieglitz M. 2008. Lability of DOC transported by Alaskan rivers to the Arctic Ocean. *Geophysical Research Letters* **35**: L03402. DOI: 10.1029/2007GL032837

Hottelet C, Braun L, Leibundgut C, Rieg A. 1993. Simulation of snowpack and discharge in an alpine karst basin. In *Snow and Glacier Hydrology, Proceedings of the Kathmandu Symposium*, Young GJ (ed). IAHS Publ: Wallingford, UK; 249–260.

Hugelius G, Tarnocai C, Broll G, Canadell JG, Kuhry P, Swanson DK. 2013. The Northern Circumpolar Soil Carbon Database: spatially distributed datasets of soil coverage and soil carbon storage in the northern permafrost regions. *Earth System Science Data* **5**: 3–13. DOI: 10.5194/essd-5-3-2013

Jutras M-F, Nasr M, Castonguay M, Pit C, Pomeroy JH, Smith TP, Zhang C, Ritchie CD, Meng F-R, Clair TA, Arp PA. 2011. Dissolved organic carbon concentrations and fluxes in forest catchments and streams: DOC-3 model. *Ecological Modelling* **222**: 2291–2313. DOI: 10.1016/j.ecolmodel.2011.03.035

Kawahigashi M, Kaiser K, Kalbitz K, Rodionov A, Guggenberger G. 2004. Dissolved organic matter in small streams along a gradient from discontinuous to continuous permafrost. *Global Change Biology* **10**: 1576–1586. DOI: 10.1111/j.1365-2486.2004.00827.x

Kicklighter DW, Hayes DJ, McClelland JW, Peterson BJ, McGuire AD, Melillo JM. 2013. Insights and issues with simulating terrestrial DOC loading of Arctic river networks. *Ecological Applications* **23**: 1817–1836.

Koch JC, Runkel RL, Striegl R, McKnight DM. 2013. Hydrologic controls on the transport and cycling of carbon and nitrogen in a boreal catchment underlain by continuous permafrost. *Journal of Geophysical Research, Biogeosciences* **118**: 698–712. DOI: 10.1002/jgrg.20058

Konz M, Seibert J. 2010. On the value of glacier mass balances for hydrological model calibration. *Journal of Hydrology* **385**: 238–246. DOI: 10.1016/j.jhydrol.2010.02.025

Krause P, Boyle D, Bäse F. 2005. Comparison of different efficiency criteria for hydrological model assessment. *Advances in Geosciences* **5**: 89–97.

Laudon H, Buttle J, Carey SK, Mcdonnell J, Mcguire K, Seibert J, Shanley J, Soulsby C, Tetzlaff D, Mcdonnell J, Mcguire K, Seibert J, Shanley J, Soulsby C, Lodge M, Creek W, Brook H. 2012. Cross-regional prediction of long-term trajectory of stream water DOC response to climate change response to climate change may be more predictable than Name. *Geophysical Research Letters* **39**: 4–9. DOI: 10.1029/2012GL053033

Lenton TM, Huntingford C. 2003. Global terrestrial carbon storage and uncertainties in its temperature sensitivity examined with a simple model. *Global Change Biology* **9**: 1333–1352. DOI: 10.1046/j.1365-2486.2003.00674.x

Lewkowicz AG, Ednie M. 2004. Probability mapping of mountain permafrost using the BTS method, Wolf Creek, Yukon Territory, Canada. *Permafrost and Periglacial Processes* **15**: 67–80. DOI: 10.1002/ppp.480

Lindström G, Johansson B, Persson M, Gardelin M, Bergström S. 1997. Development and test of the distributed HBV-96 hydrological model. *Journal of Hydrology* **201**: 272–288. DOI: 10.1016/S0022-1694(97)00041-3

Lyon SW, Mörth M, Humborg C, Giesler R, Destouni G. 2010. The relationship between subsurface hydrology and dissolved carbon fluxes for a sub-arctic catchment. *Hydrology and Earth System Sciences* **14**: 941–950. DOI: 10.5194/hess-14-941-2010

Mann PJ, Davydova A, Zimov N, Spencer RGM, Davydov S, Bulygina E, Zimov S, Holmes RM. 2012. Controls on the composition and lability of dissolved organic matter in Siberia's Kolyma River basin. *Journal of Geophysical Research* **117**: G01028. DOI: 10.1029/2011JG001798

McCartney SE, Carey SK, Pomeroy JW. 2006. Intra-basin variability of snowmelt water balance calculations in a subarctic catchment. *Hydrological Processes* **20**: 1001–1016. DOI: 10.1002/hyp.6125

McClelland JW, Stieglitz M, Pan F, Holmes RM, Peterson BJ. 2007. Recent changes in nitrate and dissolved organic carbon export from the upper Kuparuk River, North Slope, Alaska. *Journal of Geophysical Research* **112**: G04S60. DOI: 10.1029/2006JG000371

McGuire A, Anderson L. 2009. Sensitivity of the carbon cycle in the Arctic to climate change. *Ecological Monographs* **79**: 523–555.

McNamara JP, Kane DL, Hinzman LD. 1997. Hydrograph separations in an Arctic watershed using mixing model and graphical techniques. *Water Resources Research* **33**(7): 1707–1719.

Michalzik B, Tipping E, Mulder J, Lancho JFG, Matzner E, Bryant CL, Clarke N, Lofts S, Esteban MAV. 2003. Modelling the production and transport of dissolved organic carbon in forest soils. *Biogeochemistry* **66**: 241–264. DOI: 10.1023/B:BIOG.0000005329.68861.27

Neff JC, Finlay JC, Zimov SA, Davydov SP, Carrasco JJ, Schuur EAG, Davydova AI. 2006. Seasonal changes in the age and structure of dissolved organic carbon in Siberian rivers and streams. *Geophysical Research Letters* **33**: L23401. DOI: 10.1029/2006GL028222

O'Donnell JA, Jones JB. 2006. Nitrogen retention in the riparian zone of catchments underlain by discontinuous permafrost. *Freshwater Biology* **51**: 854–864. DOI: 10.1111/j.1365-2427.2006.01535.x

Oelke C, Zhang T, Serreze MC. 2004. Modeling evidence for recent warming of the Arctic soil thermal regime. *Geophysical Research Letters* **31**: n/a–n/a. DOI: 10.1029/2003GL019300

Petrone KC, Jones JB, Hinzman LD, Boone RD. 2006. Seasonal export of carbon, nitrogen, and major solutes from Alaskan catchments with discontinuous permafrost. *Journal of Geophysical Research* **111**: G02020. DOI: 10.1029/2005JG000055

Prokushkin AS, Gleixner G, McDowell WH, Ruehlow S, Schulze E-D. 2007. Source- and substrate-specific export of dissolved organic matter from permafrost-dominated forested watershed in central Siberia. *Global Biogeochemical Cycles* **21**: n/a–n/a. DOI: 10.1029/2007GB002938

Quinton WL, Hayashi M, Chasmer LE. 2011. Permafrost–thaw-induced land-cover change in the Canadian subarctic: implications for water resources. *Hydrological Processes* **25**: 152–158. DOI: 10.1002/hyp.7894

Quinton WL, Marsh P. 1999. A Conceptual Framework for Runoff Generation in a Permafrost Environment. *Hydrological Processes* **13**: 2563–2581.

Quinton WL, Shirazi T, Carey SK, Pomeroy JW. 2005. Soil water storage and active-layer development in a sub-alpine tundra hillslope, southern Yukon Territory, Canada. *Permafrost and Periglacial Processes* **16**: 369–382. DOI: 10.1002/ppp.543

R Core Team. 2012. R: a language and environment for statistical computing. R Foundation for Statistical Computing, Vienna, Austria, **2012**.

Raymond, PA, McClelland JW, Holmes RM, Zhulidov AV, Mull K, Peterson BJ, Striegl RG, Aiken GR, Gurtovaya TY. 2007. Flux and age of dissolved organic carbon exported to the Arctic Ocean: a carbon isotopic study of the five largest arctic rivers. *Global Biogeochemical Cycles* **21**. DOI: 10.1029/2007GB002934

Schaefer K, Zhang T, Bruhwiler L, Barrett A. 2011. Amount and timing of permafrost carbon release in response to climate warming. Tellus B.

Schoups G, Vrugt JA. 2010. A formal likelihood function for parameter and predictive inference of hydrologic models with correlated, heteroscedastic, and non-Gaussian errors. *Water Resources Research* **46**. DOI: 10.1029/2009WR008933

Schuur EAG, Bockheim J, Canadell JG, Euskirchen E, Field CB, Goryachkin SV, Hagemann S, Kuhry P, Lafleur PM, Lee H, Mazhitova G, Nelson FE, Rinke A, Romanovsky VE, Shiklomanov N, Tarnocai C, Venevsky S, Vogel JG, Zimov SA. 2008. Vulnerability of permafrost carbon to climate change: implications for the global carbon cycle. *Bioscience* **58**: 701. DOI: 10.1641/B580807

Smith J, Gottschalk P, Bellarby J, Chapman S, Lilly A, Towers W, Bell J, Coleman K, Nayak D, Richards M, Hillier J, Flynn H, Wattenbach M, Aitkenhead M, Yeluripati J, Farmer J, Milne R, Thomson A, Evans C, Whitmore A, Falloon P, Smith P. 2010a. Estimating changes in Scottish soil carbon stocks using ECOSSE. II. Application. *Climate Research* **45**: 193–205. DOI: 10.3354/cr00902

Smith J, Gottschalk P, Bellarby J, Chapman S, Lilly A, Towers W, Bell J, Coleman K, Nayak D, Richards M, Hillier J, Flynn H, Wattenbach M, Aitkenhead M, Yeluripati J, Farmer J, Milne R, Thomson A, Evans C, Whitmore A, Falloon P, Smith P. 2010b. Estimating changes in Scottish soil carbon stocks using ECOSSE. I. Model description and uncertainties. *Climate Research* **45**: 179–192. DOI: 10.3354/cr00899

Smith P, Smith J, Flynn H, Killham K. 2007. ECOSSE: Estimating Carbon in Organic Soils – Sequestration and Emission, Scottish Executive, Edinburgh. Edinburgh.

Striegl RG, Aiken GR, Dornblaser MM, Raymond PA, Wickland KP. 2005. A decrease in discharge-normalized DOC export by the Yukon River during summer through autumn. *Geophysical Research Letters* **32**: L21413. DOI: 10.1029/2005GL024413

Tank SE, Frey KE, Striegl RG, Raymond PA, Holmes RM, McClelland JW, Peterson BJ. 2012. Landscape-level controls on dissolved carbon flux from diverse catchments of the circumboreal. *Global Biogeochemical Cycles* **26**. DOI: 10.1029/2012GB004299

Tetzlaff D, Buttle J, Carey SK, McGuire K, Laudon H, Soulsby C. 2014. Tracer-based assessment of flow paths, storage and runoff generation in northern catchments: a review. *Hydrological Processes*. DOI: 10.1002/hyp.10412

Thornthwaite C. 1948. An approach toward a rational classification of climate. *Geographical Review* **43**: 55–94. DOI: 10.1029/2006WR005201

Tjoelker MG, Oleksyn J, Reich PB. 2001. Modelling respiration of vegetation: evidence for a general temperature-dependent Q10. *Global Change Biology* **7**: 223–230. DOI: 10.1046/j.1365-2486.2001.00397.x

Van Griensven A, Meixner T, Grunwald S, Bishop T, Diluzio M, Srinivasan R. 2006. A global sensitivity analysis tool for the parameters of multi-variable catchment models. *Journal of Hydrology* **324**: 10–23. DOI: 10.1016/j.jhydrol.2005.09.008

Wickland KP, Aiken GR, Butler K, Dornblaser MM, Spencer RGM, Striegl RG. 2012. Biodegradability of dissolved organic carbon in the Yukon River and its tributaries: seasonality and importance of inorganic nitrogen. *Global Biogeochemical Cycles* **26**. DOI: 10.1029/2012GB004342

Zambrano-Bigiarini M, Rojas R. 2013. A model-independent Particle Swarm Optimisation software for model calibration. *Environmental Modelling and Software* **43**: 5–25.

Zou L, Sun M-Y, Guo L. 2006. Temporal variations of organic carbon inputs into the upper Yukon River: evidence from fatty acids and their stable carbon isotopic compositions in dissolved, colloidal and particulate phases. *Organic Geochemistry* **37**: 944–956. DOI: 10.1016/j.orggeochem.2006.04.002

